

doi: 10.3788/gzxb20164503.0312001

相机内参量及像差系数与外参量的解耦标定方法

刘进博^{1,2}, 张小虎^{1,2}, 于起峰^{1,2}

(1 国防科学技术大学 航天科学与工程学院, 长沙 410073)

(2 图像测量与视觉导航湖南省重点实验室, 长沙 410073)

摘 要: 基于无穷远点与相机内参量关系, 提出了一种相机内参量及像差系数与外参量解耦标定方法。首先, 根据平面单应计算绝对二次曲线在像面的投影方程, 线性求解相机内参量; 然后, 将重投影点视为理想像点线性求解像差系数, 并计算像点重投影误差; 最后, 将序列图像的平面单应作为待优化参量, 以最小化像点重投影误差为目标函数, 重复上述过程, 输出最优的相机内参量和像差系数。在相同配置下, 分别对本文方法和张正友平面靶板标定方法的标定准确度进行仿真与对比分析。基于不同姿态和位置的 27 幅棋盘格图片, 分别利用这两种方法对相机内参量进行标定实验。实验结果表明: 与张正友平面靶板标定方法相比, 本文方法的标定准确度提高了至少 1%; 在实物实验中, 张正友平面靶板标定方法和本文方法的重投影残差分别为 0.064 像素和 0.008 像素。

关键词: 计算机视觉; 应用光学; 相机标定方法; 标定程序; 解耦标定; 无穷远点

中图分类号: TP187

文献标识码: A

文章编号: 1004-4213(2016)03-0312001-7

A Calibration Method for Camera Intrinsic Parameters and Image Distortion Decoupling with Extrinsic Parameters

LIU Jin-bo^{1,2}, ZHANG Xiao-hu^{1,2}, YU Qi-feng^{1,2}

(1 College of Aerospace Science and Engineering, National University of Defense Technology, Changsha 410073, China)

(2 Hunan Key Laboratory of Videometrics and Vision Navigation, Changsha 410073, China)

Abstract: Based on the relationship between infinite points and camera intrinsic parameters, a calibration method for camera intrinsic parameters and image distortion was proposed, which can realize a decoupled calibration among intrinsic parameters, image distortion and extrinsic parameters. First, solving camera intrinsic parameters from the projective equations of image of absolute quartic. Second, taking a reprojected point as an ideal image point and solving image distortion coefficient. Third, taking homography among sequence images as parameters to be optimized and taking reprojection error as cost function, then the final outputting results include camera intrinsic parameters and image distortion coefficients. Under the identical configurations, the calibration precisions of the proposed method and Zhang's method were simulated respectively and compared together. By using the 27 views of planar objects with different pose, the calibration experiment for the camera intrinsic parameters was conducted by the proposed method and Zhang's method respectively. The results show that, the calibration precision of the proposed method is improved at least 1% to compare with Zhang's method. In the calibration experiment, the reprojection error of Zhang's method and proposed method is 0.064pixel and 0.008pixel respectively.

Key words: Computer vision; Optics application; Camera calibration methods; Calibration procedures; Decoupled calibration; Infinite point

OCIS Codes: 120.4820; 150.1488; 000.2170; 110.2960

Foundation item: The National Natural Science Foundation of China (Nos. 11272347, 11072263, 11472302)

First author: LIU Jin-bo (1988—), male, Ph. D. degree, mainly focuses on computer vision. Email: liujinbo_nudt@hotmail.com

Supervisor: ZHANG Xiao-hu (1973—), male, professor, Ph. D. degree, mainly focuses on computer vision. Email: zxh1302@hotmail.com

Received: Oct. 9, 2015; **Accepted:** Dec. 23, 2015

0 Introduction

Camera calibration in photogrammetry is to solve camera intrinsic parameters, extrinsic parameters and image distortion from experiments^[1-2]. In a videometric technique and an optic technique, special equipments and spot include theodolite, collimator tube and calibration test site^[3-4]. Camera calibration has been presented since the computer vision appeared. In computer vision, a camera calibration process is accomplished through analyzing captured images. Current camera calibration methods can be classified into 3 categories; traditional camera calibration methods, camera calibration methods based on active vision and camera self-calibration methods.

Traditional camera calibration methods use scene information, includes control points or lines with accurate coordinates, to solve camera intrinsic and extrinsic parameters. Traditional camera calibration methods can be classified into 3 categories: 1) Nonlinear optimization method. The relationship between 3-D control points and its corresponding image points is nonlinear. So, firstly, the cost function should be constructed and then optimized. Most methods in photogrammetry are belonging to this category^[5-7]. 2) Direct linear transformation method(DLT). DLT was proposed by Abdel and Karara^[8]. DLT methods are fast, but neglect the image distortion and the constraint relationship among parameters. So, the precision of DLT methods is low. 3) Two-step methods. These methods solve most parameters by DLT and other parameters by nonlinear or iterative optimization algorithms. Among all the two-step methods, Tsai calibration method and Weng calibration method are most typical^[9-10].

Camera self-calibration methods only use the relationship among sequence images to solve camera intrinsic and extrinsic parameters in a difference of a scale factor related to real results^[11-12]. Self-calibration methods need no initial value, so they are different from most optimization algorithms needing initial value, *e. g.* bundle adjustment. Camera self-calibration methods are frontiers of modern science and technology. Fraugeras first proposed the idea of self-calibration methods and introduced Kruppa equation describing constraint relationship among sequence images, making camera self-calibration with general motion possibility^[13]. For the given difficulties of directly solving Kruppa equation, many researchers proposed the step-by-step calibration methods.

Camera calibration methods based on an active computer vision require camera do some controllable

motion, *e. g.* rotating around optical center and translation merely^[14-15]. With the particularity of controllable motion, camera intrinsic and extrinsic parameters can be solved. During a process of hand-eye calibration, the motion of camera can be controlled accurately, and therefore these methods are used frequently.

The precision of camera intrinsic parameters, not extrinsic parameters, is a key factor affecting measuring precision of vehicle-theodolite's platform vibration^[16]. However, most calibration methods solve intrinsic parameters and extrinsic parameters simultaneously. In order to decrease the reprojection error, it needs to optimize intrinsic parameters and extrinsic parameters. In this case, the reprojection error caused by an extrinsic calibration error can be adjusted to intrinsic parameters, increasing intrinsic parameters' error. For this particular requirement, a calibration method for camera intrinsic parameters and image distortion based on planar target was proposed in this paper, which can realize decoupled calibration among intrinsic parameters and extrinsic parameters.

1 Calibration method for camera intrinsic and image distortion

The key idea and principle is that: First, solving intrinsic parameters from the projective equations of image of absolute quartic. Second, taking a reprojected point as an ideal image point and solving image distortion coefficient. Third, taking homography among sequence images as parameters to be optimized and taking reprojection error as cost function, then outputting final results including camera intrinsic parameters and image distortion coefficients.

1.1 Theory of camera intrinsic parameters calibration

Absolute quartic Ω_∞ is a quartic on infinite plane. In a reference coordinate $\pi_\infty = (0, 0, 0, 1)$ and point $\mathbf{X} = (X_1, X_2, X_3, X_4)$ on Ω_∞ satisfies

$$\left. \begin{aligned} x_1^2 + x_2^2 + x_3^2 \\ x_4^2 \end{aligned} \right\} = 0 \quad (1)$$

Ω_∞ can be defined as

$$(x_1 \ x_2 \ x_3) \Omega_\infty (x_1 \ x_2 \ x_3)^T = 0 \quad (2)$$

From Eq. (2), Ω_∞ is a quartic consists of circular points. $(1 \pm i \ 0)^T$ is two intersection points of all spatial circles and Ω_∞ .

Point \mathbf{X}_∞ on π_∞ can be written as $\mathbf{X}_\infty = (d^T, 0)^T$ and note its correspondence image point as \mathbf{x}

$$\mathbf{x} = \mathbf{P}\mathbf{X}_\infty = \mathbf{K}\mathbf{R}[\mathbf{I} | -\mathbf{C}] \begin{pmatrix} d \\ 0 \end{pmatrix} = \mathbf{K}\mathbf{R}d = \mathbf{H}d \quad (3)$$

where \mathbf{P} is a projection matrix. \mathbf{K} is a camera intrinsic matrix. \mathbf{R} is a rotation matrix from reference coordinate system to camera coordinate system. \mathbf{H} is a homograph

transforming infinite plane to image plane.

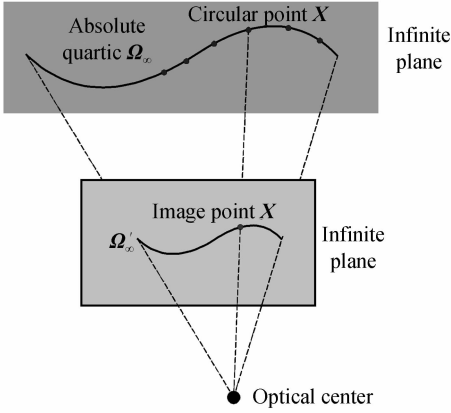


Fig. 1 Absolute quartic and its projection on image plane

Under the condition of point transformation $\mathbf{x} = \mathbf{H}\mathbf{d}$, quadratic transformation can be derived as

$$\mathbf{d}^T \boldsymbol{\Omega}_{\infty} \mathbf{d} = (\mathbf{H}^{-1} \mathbf{x})^T \boldsymbol{\Omega}_{\infty} (\mathbf{H}^{-1} \mathbf{x}) = \mathbf{x}^T (\mathbf{H}^{-T} \boldsymbol{\Omega}_{\infty} \mathbf{H}^{-1}) \mathbf{x} = \mathbf{x}^T \boldsymbol{\Omega}'_{\infty} \mathbf{x} \quad (4)$$

Substitute $\mathbf{H} = \mathbf{K}\mathbf{R}$ into Eq. (4).

$$\boldsymbol{\Omega}'_{\infty} = (\mathbf{K}\mathbf{R})^{-T} \boldsymbol{\Omega}_{\infty} (\mathbf{K}\mathbf{R})^{-1} = \mathbf{K}^{-T} (\mathbf{R}^{-T} \mathbf{I} \mathbf{R}^{-1}) \mathbf{K}^{-1} = (\mathbf{K}\mathbf{K}^T)^{-1} \quad (5)$$

The projection of spatial conic $\boldsymbol{\Omega}_{\infty}$ on image is noted as $\boldsymbol{\Omega}'_{\infty}$. Once $\boldsymbol{\Omega}'_{\infty}$ is identified, camera intrinsic parameters can be obtained by Cholesky matrix decomposition.

The quadratic equation is represented by nonhomogeneous coordinates.

$$ax^2 + bxy + cy^2 + dx + ey + f = 0 \quad (6)$$

Eq. (6) is rewritten as a matrix form.

$$\mathbf{x}^T \boldsymbol{\Omega}'_{\infty} \mathbf{x} = 0 \quad (7)$$

And

$$\boldsymbol{\Omega}'_{\infty} = \begin{pmatrix} a & b/2 & d/2 \\ b/2 & c & e/2 \\ d/2 & e/2 & f \end{pmatrix}$$

Quadratic curve has 5 freedom and 5 general points can define a conic uniquely. As analyzed above, we know that arbitrary plane intersect absolute conic with 2 circular points. Note transformation from plane $\boldsymbol{\pi}_i$ to image plane as \mathbf{H}_i . The projection on image of circular point is written as

$$\mathbf{p}_i^l = \begin{pmatrix} x_i^l \\ y_i^l \\ 1 \end{pmatrix} = \mathbf{H}_i \begin{pmatrix} 1 \\ i \\ 0 \end{pmatrix}, \quad \mathbf{p}_i^r = \begin{pmatrix} x_i^l \\ y_i^l \\ 1 \end{pmatrix} = \mathbf{H}_i \begin{pmatrix} 1 \\ -i \\ 0 \end{pmatrix}$$

Substitute it into Eq. (4)

$$\begin{pmatrix} (x_1^l)^2 & x_1^l y_1^l & (y_1^l)^2 & x_1^l & y_1^l & 1 \\ (x_2^l)^2 & x_2^l y_2^l & (y_2^l)^2 & x_2^l & y_2^l & 1 \\ \vdots & \vdots & \vdots & \vdots & \vdots & \vdots \\ (x_{n-1}^l)^2 & x_{n-1}^l y_{n-1}^l & (y_{n-1}^l)^2 & x_{n-1}^l & y_{n-1}^l & 1 \\ (x_n^l)^2 & x_n^l y_n^l & (y_n^l)^2 & x_n^l & y_n^l & 1 \end{pmatrix} \cdot \mathbf{c} = 0 \quad (8)$$

And

$$\mathbf{c} = (a \quad b \quad c \quad d \quad e \quad f)^T$$

Projection equation of absolute conic can be solved uniquely on condition that there are more than 2 planes in space.

1.2 Calibration for image distortion based on point correspondence

Without loss of generality, only considering frame # i in sequence images, the relationship between ideal image point $\tilde{\mathbf{p}}_j^i$ and spatial point \mathbf{P}_j can be written as

$$\tilde{\mathbf{p}}_j^i = \mathbf{H}_i \mathbf{P}_j \quad (9)$$

Considering D. C. Brown image distortion model, real image point and ideal image point has the following relationship

$$\tilde{\mathbf{p}}_j^i = [1 + k_0 (r_j^i)^2 + k_1 (r_j^i)^4 + k_4 (r_j^i)^6] \mathbf{p}_j^i + \begin{Bmatrix} 2k_2 x_j^i y_j^i + k_3 [(r_j^i)^2 + 2(x_j^i)^2] \\ 2k_3 x_j^i y_j^i + k_2 [(r_j^i)^2 + 2(y_j^i)^2] \end{Bmatrix} \quad (10)$$

And

$$(r_j^i)^2 = (x_j^i)^2 + (y_j^i)^2$$

where k_0, k_1, k_2, k_3, k_4 are image distortion coefficients. Eq. (10) is written as a homogeneous linear equation on image distortion coefficients.

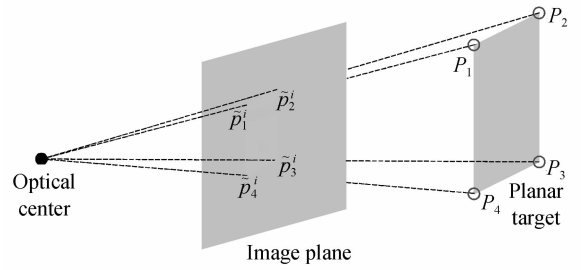


Fig. 2 Point correspondence between space and image

Suppose that there are n images and each image has m correspondences. Homogeneous linear equations can be written as

$$\mathbf{A}_{m \times n} \mathbf{k}_{5,1} = \mathbf{B}_{m \times n,1} \quad (11)$$

Eq. (11) is solved by least square method.

1.3 Iterative optimization method

Without loss of generality, only considering i -th frame and computing reprojection error e_i .

Note image point deleted distortion as $\hat{\mathbf{p}}_j^i$, then

$$\hat{\mathbf{p}}_j^i = [1 + k_0 (r_j^i)^2 + k_1 (r_j^i)^4 + k_4 (r_j^i)^6] \mathbf{p}_j^i + \begin{Bmatrix} 2k_2 x_j^i y_j^i + k_3 [(r_j^i)^2 + 2(x_j^i)^2] \\ 2k_3 x_j^i y_j^i + k_2 [(r_j^i)^2 + 2(y_j^i)^2] \end{Bmatrix} \quad (12)$$

Reprojective image point $\tilde{\mathbf{p}}_j^i$ is expressed as

$$\tilde{\mathbf{p}}_j^i = \mathbf{H}_i \mathbf{P}_j$$

The reprojection error is defined as

$$e(\mathbf{H}) = \sum_{i=1}^n \sum_{j=1}^m d(\hat{\mathbf{p}}_j^i, \tilde{\mathbf{p}}_j^i)^2 \quad (13)$$

The problem of computing homograph is changed into a problem of optimization:

$$\mathbf{H}_{\text{opt}} = \min e(\mathbf{H})$$

Finally, the optimal camera intrinsic parameters and image distortion coefficients are solved through § 1.1 and § 1.2.

2 Experiments

Experiments include 2 parts, simulations and physical experiments.

Experiments mainly consider two calibration methods, Zhang's calibration method based on planar target^[17] and our method. Zhang's method is proposed by "camera calibration toolbox for matlab-Jean-Yves bouguet".

2.1 Simulations

Extraction noise, position noise and image number are three factors of calibration precision. For these 3 factors, we design 3 simulations individually. In these simulation models, camera resolution is 1024×1024 pixel and equivalent focal length is 2 700 pixel. Fig. 4 is

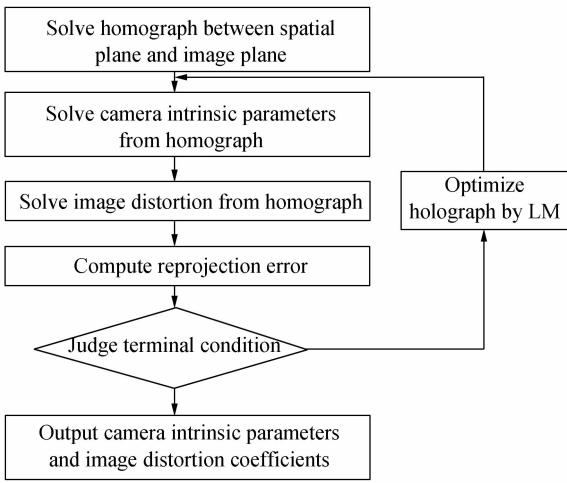
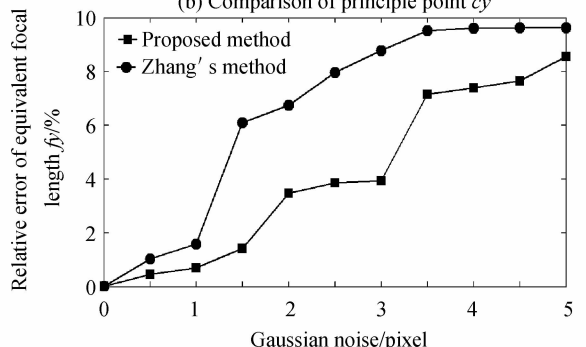
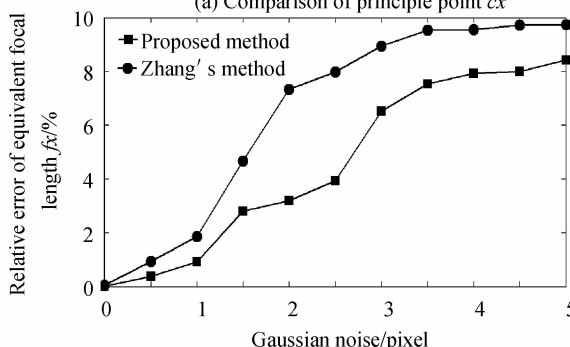
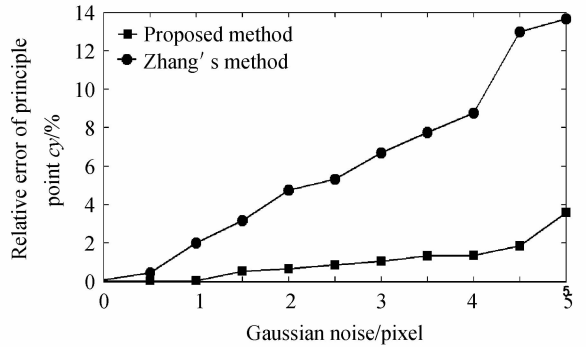
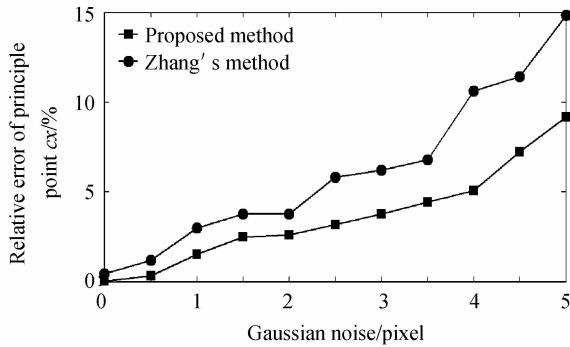


Fig. 3 Flowchart of proposed decoupled calibration method



(c) Comparison of equivalent focal length f_x

(d) Comparison of equivalent focal length f_y

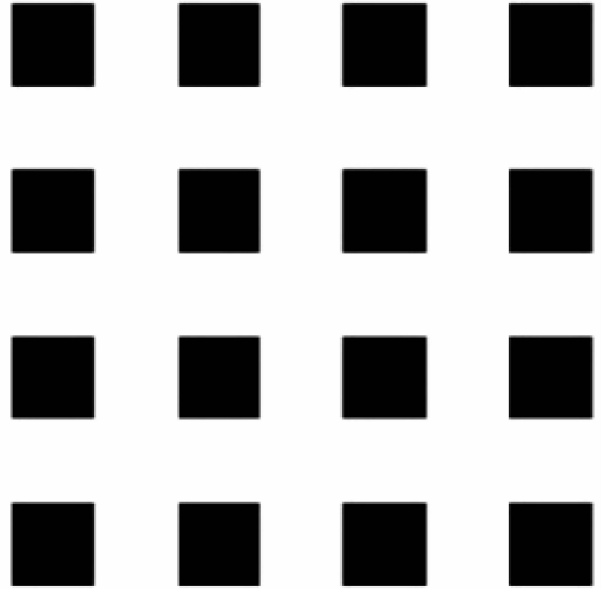
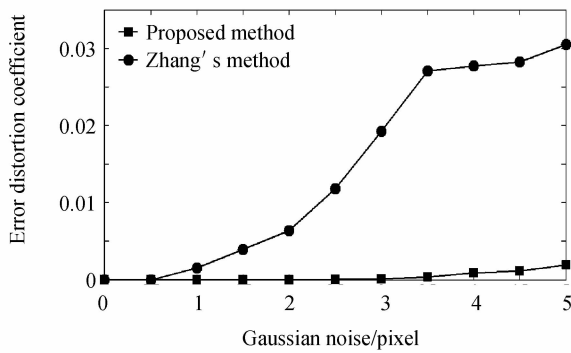


Fig. 4 Simulated planar target

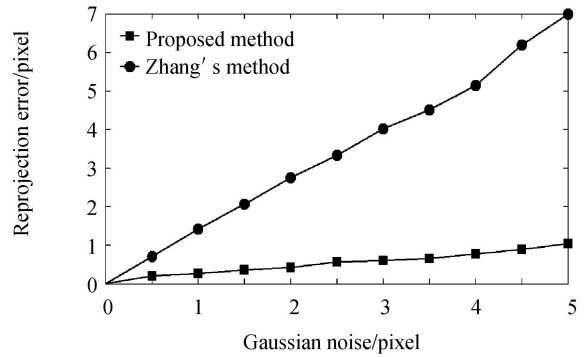
simulated planar target consisting of 16 squares. Size of every square is $20 \text{ mm} \times 20 \text{ mm}$. Each condition is simulated 100 times.

1) Extraction noise

In this simulation, there are 6 images and each image has 64 control points. Add different Gaussian noise into image. Compare our method with Zhang's method by calibration results and compute calibration error. The results show that: 1) Our method is superior to Zhang's method under same extraction noise. 2) The calibration error is increasing with the increase of extraction noise.



(e) Comparison of distortion coefficient



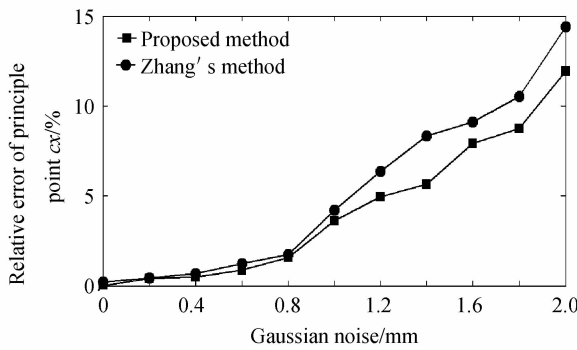
(f) Comparison of reprojection error

Fig. 5 Relationship between calibration error and extraction noise

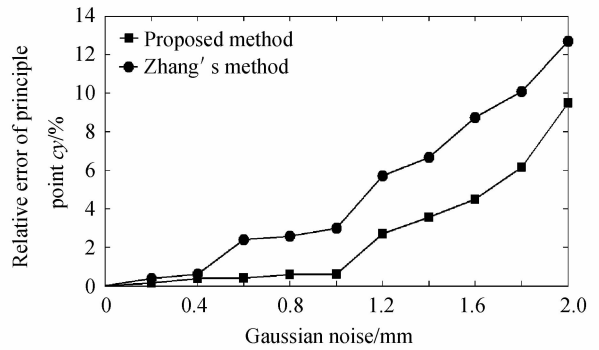
2) Position noise

In this simulation, there are 6 images and each image has 64 control points. Adding different Gaussian noise into control points. To compare our method with Zhang's method by calibration result and compute the

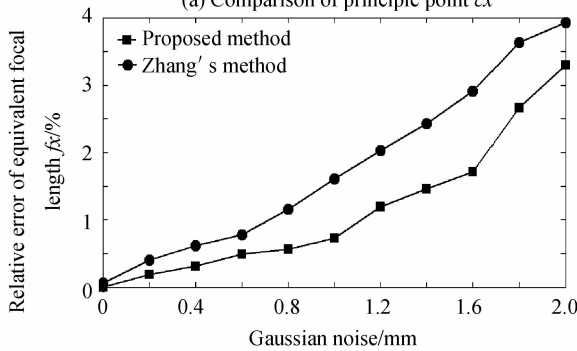
calibration error. The results show that: 1) Our method is superior to Zhang's method under same space point position noise condition. 2) Calibration error is increasing with the increase of position noise.



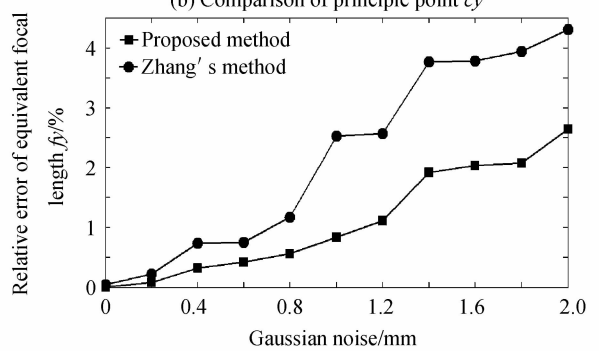
(a) Comparison of principle point c_x



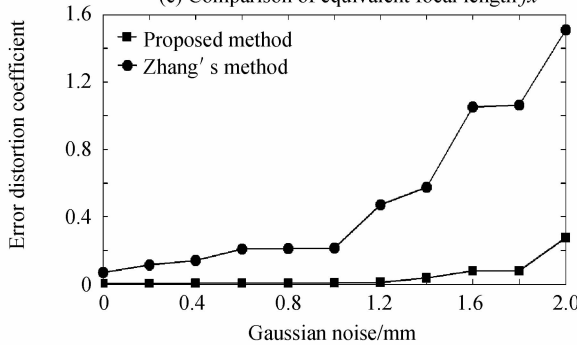
(b) Comparison of principle point c_y



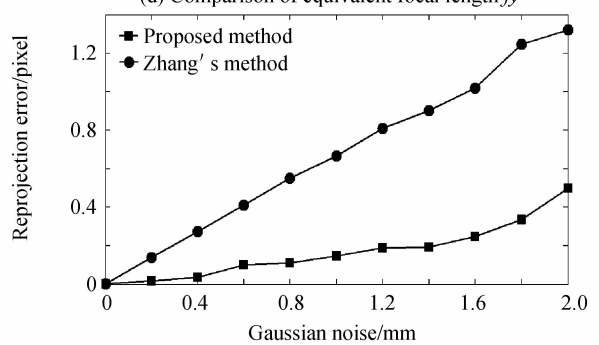
(c) Comparison of equivalent focal length f_x



(d) Comparison of equivalent focal length f_y



(e) Comparison of distortion coefficient



(f) Comparison of reprojection error

Fig. 6 Relationship between calibration error and position noise

3) Number of images

In this simulation, adding Gaussian noise with

mean value of 0 and standard deviation of 0.5 into control points and image points. Each image has 64

control points. The number of images increases from 6 to 20. To compare our method with Zhang's method by calibration result and compute calibration error. The results show that; 1) Our method is superior to Zhang's

s method under same number of images condition. 2) Calibration error is decreasing with image number ranged from 6~20.

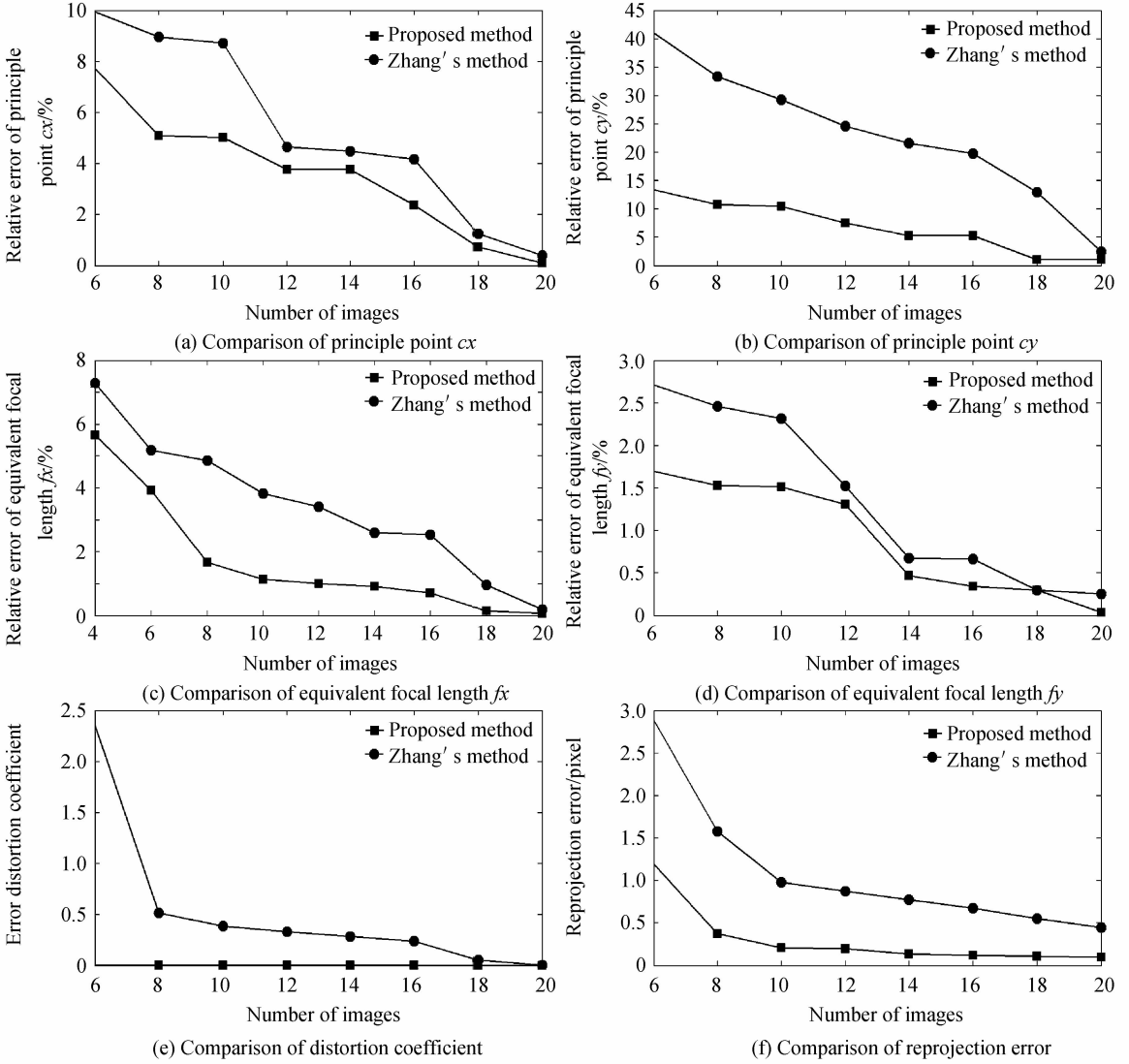


Fig. 7 Relationship between calibration error and number of images

2.2 Physical experiment

Planar target is a glass chessboard with 484 corner points. Each square's size is $15\text{mm} \times 15\text{mm}$. Camera type is IMPERX IGV-B2520 with resolution of $2456\text{ pixel} \times 2058\text{ pixel}$. Focal length is 50 mm and pixel size is $3.45\text{ }\mu\text{m} \times 3.45\text{ }\mu\text{m}$.

We captured 27 images with different pose. To use Zhang's method and our method solve camera intrinsic parameters and image distortion coefficients. Table. 1 is shown results, which indicate that; 1) Our method is improved to a large extent in terms of reprojection error. 2) Principle point calibrated by our method is closer to nominal values, while equivalent focal length calibrated by our method is further away from nominal values. The reason is that; 1) Nominal value is not true result. Assembly error cannot be

neglected. 2) Cost function based on reprojection error is not convex and this may lead to a locally optimal solution.

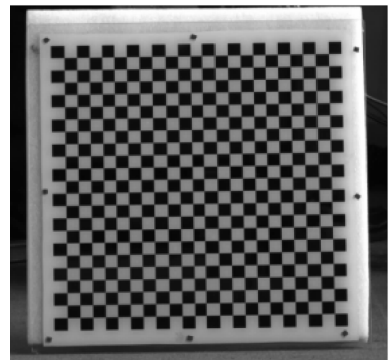


Fig. 8 Glass chessboard

Table 1 Calibration results of physical experiment

	Principle		Equivalent focal		Image distortion	Reprojection
	point/pixel		length/pixel		coefficient	error/pixel
	cx	cy	fx	fy	k_0	e
Zhang's Method	1 160.4	776.2	14 590.7	14 618.9	-0.051	0.064
Proposed method	1 180.3	10 97.9	14 860.1	14 779.8	0.008	0.008
Nominal values	1 228.0	1 029.0	14 492.7	14 492.7		

3 Conclusions

The precision of camera intrinsic parameters and image distortion is a key factor of measuring vehicle-theodolite platform vibration. For the special working environment of vehicle-theodolite, we proposed a calibration method for camera intrinsic parameters and image distortion, which can realize a decoupled calibration among intrinsic parameters and extrinsic parameters. According to the research in the paper, the main conclusions are that the calibration error is increasing with the increase of the extraction noise and the position noise respectively and decreasing related to image number ranged from 6~20. The same as Zhang's method, our method is also an off-line calibration method, cannot be applied in real-time systems.

Reference

[1] SHANG Y, YU Q F, ZHANG X H. Analytical method for camera calibration from a single image with four coplanar control lines[J]. *Applied Optics*, 2004, **43**(28): 5364-5368.

[2] ZHAO R J, LIU E H, ZHANG W M. Measurement of 3D pose of objects based on weak perspective model[J]. *Acta Photonica Sinica*, 2014, **43**(5): 0512002.

[3] XU C, GAO H. The attitude angle estimation-based distance measurement of tank target in monocular image[J]. *Acta Photonica Sinica*, 2015, **44**(5): 0512002.

[4] YU Q F, SUN X Y, JIANG G W. Relay camera videometrics based conversion method for unstable platform to static reference[J]. *Science China Technique Science*, 2011, **54**: 1017-1023.

[5] LIU J B, ZHANG X H, LIU H B, et al. New method for camera pose estimation based on line correspondence[J]. *Science China Technique Science*, 2013, **56**: 2787-2797.

[6] SHANG Y, YU Q F, ZHANG X H, et al. Analytical method

for camera calibration from a single image with four coplanar control lines[J]. *Applied Optics*, 2004, **43**: 5364-5368.

[7] ZHANG X H, ZHANG Z, LI Y, et al. Robust camera pose estimation from unknown or known line correspondences[J]. *Applied Optics*, 2012, **51**: 936-948.

[8] HU M L. Space and transformation[M]. Beijing: Science Press, 2009.

[9] HARTLEY R, ANDREW Z. Multiple view geometry in computer vision[M]. Hefei: Anhui University Press, 2002.

[10] YU Q F, SHANG Y. Videometrics: principles and researches[M]. Beijing: Science Press, 2009.

[11] TARDIF J P, STURM P, ROY S. Plane-based self-calibration of radial distortion[C]. Proceeding of the Eleventh IEEE International Conference on Computer Vision, 2007: 1-8.

[12] LV F, ZHAO T, NEVATIA R. Camera calibration from video of a walking human[J]. *IEEE Transactions on Pattern Analysis and Machine Intelligence*, 2006, **28**(9): 1513-1518.

[13] QI F. Constraints on general motions for camera calibration with one-dimensional objects[J]. *Pattern Recognition*, 2007, **40**(6):1785-1792.

[14] LI Y F, CHEN S Y. Automatic recalibration of an active structured light vision system[J]. *IEEE Transactions on Robotics and Automation*, 2003, **19**(2): 259-268

[15] HUANG H Y, QI F H. A genetic algorithm approach to accurate calibration of camera[J]. *Journal of Infrared Millimeter Waves*, 2000, **19**(1): 1-6.

[16] LIU J B, ZHANG X H, LIU H B, et al. Correction method for non-landing measuring of vehicle-mounted theodolite based on static datum conversion [J]. *Science China Technique Science*, 2013, **56**: 2268-2277.

[17] ZHANG Z Y. A flexible new technique for camera calibration[J]. *IEEE Transactions on Pattern Analysis and Machine Intelligence*, 2000, **22**(11): 1330-1334.